

University of Nebraska - Lincoln

DigitalCommons@University of Nebraska - Lincoln

---

Papers in Natural Resources

Natural Resources, School of

---

2009

## Characterizing the Seasonal Dynamics of Plant Community Photosynthesis Across a Range of Vegetation Types

Lianhong Gu

*Oak Ridge National Laboratory, lianhong-gu@ornl.gov*

Wilfred M. Post

*Oak Ridge National Laboratory, wmp@ornl.gov*

Dennis D. Baldocchi

*University of California-Berkeley, baldocchi@berkeley.edu*

T. Andrew Black

*University of British Columbia, ablack@interchange.ubc.ca*

Andrew E. Suyker

*University of Nebraska - Lincoln, asuyker1@unl.edu*

*See next page for additional authors*

Follow this and additional works at: <https://digitalcommons.unl.edu/natrespapers>



Part of the [Natural Resources and Conservation Commons](#)

---

Gu, Lianhong; Post, Wilfred M.; Baldocchi, Dennis D.; Black, T. Andrew; Suyker, Andrew E.; Verma, Shashi; Timo Vesala; and Wofsy, Steve C., "Characterizing the Seasonal Dynamics of Plant Community Photosynthesis Across a Range of Vegetation Types" (2009). *Papers in Natural Resources*. 174. <https://digitalcommons.unl.edu/natrespapers/174>

This Article is brought to you for free and open access by the Natural Resources, School of at DigitalCommons@University of Nebraska - Lincoln. It has been accepted for inclusion in Papers in Natural Resources by an authorized administrator of DigitalCommons@University of Nebraska - Lincoln.

---

**Authors**

Lianhong Gu, Wilfred M. Post, Dennis D. Baldocchi, T. Andrew Black, Andrew E. Suyker, Shashi Verma, Timo Vesala, and Steve C. Wofsy

# Characterizing the Seasonal Dynamics of Plant Community Photosynthesis Across a Range of Vegetation Types

Lianhong Gu, Wilfred M. Post, Dennis D. Baldocchi, T. Andrew Black, Andrew E. Suyker, Shashi B. Verma, Timo Vesala, and Steve C. Wofsy

**Abstract** The seasonal cycle of plant community photosynthesis is one of the most important biotic oscillations to mankind. This study built upon previous efforts to develop a comprehensive framework to studying this cycle systematically with eddy covariance flux measurements. We proposed a new function to represent the cycle and generalized a set of phenological indices to quantify its dynamic characteristics. We suggest that the seasonal variation of plant community photosynthesis generally consists of five distinctive phases in sequence each of which results from the interaction between the inherent biological and ecological processes and the progression of climatic conditions and reflects the unique functioning of plant community at different stages of the growing season. We applied the improved methodology to seven vegetation sites ranging from evergreen and deciduous forests to crop to grasslands and covering both cool-season (vegetation active during cool months,

---

L. Gu (✉) and W.M. Post

Environmental Sciences Division, Oak Ridge National Laboratory, Oak Ridge, TN, USA  
e-mail: lianhong-gu@ornl.gov and wmp@ornl.gov

D.D. Baldocchi

Department of Environmental Science, Policy and Management, University of California Berkeley, CA, USA  
e-mail: baldocchi@nature.berkeley.edu

T.A. Black

Land and Food Systems, University of British Columbia, Vancouver, BC, USA  
e-mail: ablack@interchange.ubc.ca

A.E. Suyker and S.B. Verma

School of Natural Resources, University of Nebraska Lincoln, Lincoln, NE, USA  
e-mail: asuyker1@unl.edu and svermal1@unl.edu

T. Vesala

Department of Physics, University of Helsinki, Helsinki, Finland  
e-mail: timo.vesala@helsinki.fi

S.C. Wofsy

Atmospheric and Environmental Sciences, Harvard University, Cambridge, MA, USA  
e-mail: scw@io.harvard.edu

e.g. Mediterranean climate grasslands) and warm-season (vegetation active during warm months, e.g. temperate and boreal forests) vegetation types. Our application revealed interesting phenomena that had not been reported before and pointed to new research directions. We found that for the warm-season vegetation type, the recovery of plant community photosynthesis at the beginning of the growing season was faster than the senescence at the end of the growing season while for the cool-season vegetation type, the opposite was true. Furthermore, for the warm-season vegetation type, the recovery was closely correlated with the senescence such that a faster photosynthetic recovery implied a speedier photosynthetic senescence and vice versa. There was evidence that a similar close correlation could also exist for the cool-season vegetation type, and furthermore, the recovery-senescence relationship may be invariant between the warm-season and cool-season vegetation types up to an offset in the intercept. We also found that while the growing season length affected how much carbon dioxide could be potentially assimilated by a plant community over the course of a growing season, other factors that affect canopy photosynthetic capacity (e.g. nutrients, water) could be more important at this time scale. These results and insights demonstrate that the proposed method of analysis and system of terminology can serve as a foundation for studying the dynamics of plant community photosynthesis and such studies can be fruitful.

## 1 Introduction

The dynamics of plant community photosynthesis consists of diurnal and seasonal cycles. These two cycles are the most important biotic oscillations to mankind. The diurnal photosynthetic cycle is primarily driven by changes in light availability associated with the rotation of the Earth and is thus relatively predictable. The seasonal cycle, however, is more complex. It is a process orchestrated by internal biological mechanisms and driven by systematic changes in a suite of interdependent environmental factors such as temperature, photoperiod, radiation, moisture, and nutrient availability. The study of the plant community photosynthetic cycle at the seasonal time scale can be considered as an extension of plant phenology (Gu et al. 2003a; also see the Preface of current volume). This extension, or “vegetation photosynthetic phenology”, represents the functional aspect of plant phenology while traditional plant phenological studies focus on the structural aspect such as budbreak, flowering, leaf coloring and leaf fall. Research on vegetation photosynthetic phenology can enrich the ancient but revived discipline of phenology so that it can become a truly integrative environmental science (Schwartz 2003).

The advance of the eddy covariance technique (Baldocchi et al. 1988; Baldocchi 2003) provides a tool amenable for studying the dynamics of plant community photosynthesis (Falge et al. 2002; Gu et al. 2002, 2003a, b). Global and regional networks of eddy covariance flux tower sites covering a wide range of vegetation types have been formed (Baldocchi et al. 2001; Gu and Baldocchi 2002). Although an eddy covariance system measures only the difference between the gross photosynthesis of the plant community and ecosystem respiration (the net ecosystem exchange,

NEE, of  $\text{CO}_2$ ), NEE can be partitioned using approaches such as response functions (Gu et al. 2002), isotopic analysis (Bowling et al. 2001) and simultaneous measurements of carbonyl sulfide flux (Campbell et al. 2008). Thus there exists a great potential of using flux networks to investigate the dynamics of plant community photosynthesis at multiple time scales. When such investigation is conducted in conjunction with examination of variations in plant community structures, underlying biochemical and physiological processes, and climatic conditions, mechanisms controlling the biological oscillations most important to mankind can be revealed. These efforts could not only enhance the theoretical bases of global change biology and ecology and but also lead to effective tools for terrestrial ecosystem management.

This chapter has two objectives. The first is to describe the improvement we have made to the analytical framework of plant community photosynthesis developed in Gu et al. (2003a). The second is to present the application of the improved framework to an expanded set of vegetation sites. Our effort to improve the methodology was guided by three requirements: easy implementation, general applicability, and straightforward link to ecophysiological processes. The application was conducted to examine how the concepts and method of analysis developed in Gu et al. (2003a) and refined in current study could be used to reveal the dynamics and control of the vegetation photosynthetic cycle. To this end, we analyzed the factors affecting the potential of gross primary production at the seasonal time scale. We were particularly interested in the photosynthetic recovery at the beginning and the photosynthetic senescence at the end of the growing season and how recovery and senescence might be related to each other. Instead of presenting site-specific findings, we focused on emergent, community-level photosynthetic properties across vegetation types.

## 2 Sites and Data Used in the Present Study

We used data from seven eddy covariance flux sites for analyses conducted in the present paper, including five warm-season (vegetation active during warm months) and two cool-season (active during cool months) vegetation sites. The five warm-season sites were a Scots pine forest in Hyytiälä, Finland ( $61^{\circ}51'N$ ,  $24^{\circ}17'E$ ; data from 1997; Rannik et al. 2000), an aspen forest in Prince Albert National Park, Saskatchewan, Canada ( $53^{\circ}63'N$ ,  $106^{\circ}20'W$ ; data from 1996; Black et al. 2000), a mixed deciduous forest in Walker Branch Watershed in Tennessee, USA ( $35^{\circ}58'N$ ,  $84^{\circ}17'W$ ; data from 1996; Wilson et al. 2000), a mixed hardwood forest in Massachusetts, USA (Harvard Forest,  $42^{\circ}32'N$ ,  $72^{\circ}10'W$ ; data from 1992; Goulden et al. 1996), and a native tallgrass prairie in Okalahoma, USA ( $36^{\circ}56'N$ ,  $96^{\circ}41'W$ ; data from 1997; Suyker and Verma 2001). These five sites were also used in Gu et al. (2003a). The two cool-season sites were a winter wheat site in Okalahoma, USA ( $36^{\circ}45'N$ ,  $97^{\circ}05'W$ ; data from 1997; Burba and Verma 2005) and a grassland site in northern California, USA ( $38^{\circ}25'N$ ,  $120^{\circ}57'W$ ; data from 2001; Baldocchi et al. 2004). For details of these sites, please see the citations listed.

Our analysis was based on canopy photosynthetic rates which were derived from NEE in the same way as described in detail in Gu et al. (2002) and Gu et al.

(2003a, b) except for the Harvard Forest site. Harvard Forest Data Archive (<http://harvardforest.fas.harvard.edu/data/archive.html>) provided values of the gross ecosystem exchange (i.e. the canopy photosynthetic rate as termed here). The Harvard Forest group calculated the gross ecosystem exchange in a similar fashion (i.e. response functions based on temperature and photosynthetically active radiation, see the documentation in the Harvard Forest website). Therefore data from all sites were processed consistently and are thus comparable. The partitioning of NEE avoided some processes important at short time scales including, for example, the influence of soil moisture and newly assimilated photosynthate on soil efflux (e.g. Liu et al. 2006). These omissions, however, do not affect the objectives of this paper which are interested in patterns occurring at the seasonal time scale.

### 3 Representation of the Seasonal Dynamics of Plant Community Photosynthesis

The seasonal cycle of plant community photosynthesis is described by the temporal variation of the canopy photosynthetic capacity (CPC). The CPC is defined as the maximal gross photosynthetic rate at the canopy level when the environmental conditions (e.g. light, moisture, and temperature) are non-limiting for the time of a year under consideration. This definition takes into account the seasonal variation in climate and thus is different from the definition of the leaf-level photosynthetic capacity, which generally assumes that the light intensity is at a saturating level (i.e.  $> 1,000 \mu\text{mol photons m}^{-2} \text{s}^{-1}$ ) and temperature is about  $25^\circ\text{C}$  regardless of the season under consideration. In contrast, the environmental conditions under which a particular value of the CPC is realized depend on the time of the year.

The CPC forms the boundary line in the scatter plot of the instantaneous canopy photosynthetic rate against time, assuming data from the whole year are used. In practice, the instantaneous canopy photosynthetic rate is derived from NEE measurements which are generally at an hourly or half-hourly resolution. The boundary line can be adequately represented by the following composite function:

$$A(t) = y_0 + \frac{a_1}{\left[1 + \exp\left(-\frac{t-t_{01}}{b_1}\right)\right]^{c_1}} - \frac{a_2}{\left[1 + \exp\left(-\frac{t-t_{02}}{b_2}\right)\right]^{c_1}} \quad (1)$$

where  $A(t)$  is the CPC in day  $t$ ;  $y_0$ ,  $a_1$ ,  $a_2$ ,  $b_1$ ,  $b_2$ ,  $c_1$ ,  $c_1$ ,  $t_{01}$ , and  $t_{02}$  are empirical parameters to be estimated. As shown later, the new function (Eqn. 1) is extremely flexible and can fit well diverse seasonal cycles of plant community photosynthesis. It is capable of simultaneously representing both the recovery and senescence parts of the growing season. In contrast, the Weibull function of Gu et al. (2003a) treats the two parts separately, creating a discontinuity in the middle of the growing season. The new function also eliminates the IF-THEN condition in the Weibull function, and thus its empirical parameters can be estimated with optimization

algorithms that require derivatives (the IF-THEN condition leads to discontinuity in derivatives).

To estimate the parameters in Eqn. (1) from NEE measurements, we use the following iterative procedures:

- a. Compute hourly or half-hourly (depending on observational time steps) canopy photosynthetic rates from NEE measurements
- b. Select the largest value from each day to form a time series of the daily maximal canopy photosynthetic rate. The time series shall cover the complete seasonal cycle.
- c. Fit Eqn. (1) to the obtained time series.
- d. For each point in the time series, compute the ratio of the daily maximal canopy photosynthetic rate to the value predicted by Eqn. (1) for the corresponding day with the fitted parameters.
- e. Conduct the Grubb's test (NIST/SEMATECH 2006) to detect if there is an outlier in the obtained ratios.
- f. If an outlier is detected, remove this outlier and go to Step c.
- g. If no outlier is found, remove the data points whose ratios are at least one standard deviation ( $1\sigma$ ) less than the mean ratio. The remaining dataset is considered to consist of the canopy photosynthetic capacity at various times of the growing season.
- h. Fit Eqn. (1) to the time series of the CPC. Eqn. (1) with the obtained parameters depict the seasonal cycle of plant community photosynthesis and is then used for further analyses (see the next section).

The automated, rigorous statistical procedures outlined above improves on the subjective, visual approach of Gu et al. (2003a). In the new approach, the outlier test and identification of data representing the seasonal cycle of plant community photosynthesis are done through the ratio of the daily maximal canopy photosynthetic rate to the value of canopy photosynthetic capacity predicted by Eqn. (1) in each iteration. This normalization process prevents potential bias in the fitting by eliminating the influence of the systematic temporal variation in the canopy photosynthetic capacity on the testing statistics. We conduct the outlier test out of a concern that a few outliers may greatly distort the fitted seasonal pattern of plant community photosynthesis. The Grubb's test has to be done one point at a time, that is, each time an outlier is found, Eqn. (1) must be readjusted (refit) to remove the effect of this identified outlier. This requirement leads to the iteration between Steps c and f. The outliers detected through this iteration are either of unusually low values which may occur in days with severe, photosynthesis-inhibiting weather conditions, or unreasonably large values which may result from noise in the original NEE measurements. Overall, outliers are few (Figs. 1 and 2).

The dataset free of outliers may still contain fairly low values of daily maximal canopy photosynthetic rates that result from short-term, suppressive weather conditions such as heavy cloud cover which are not part of the climate forcing that drives the seasonal photosynthetic cycle. Therefore, after the outliers are detected and removed, we further examine the deviation of the ratio of the daily maximal canopy

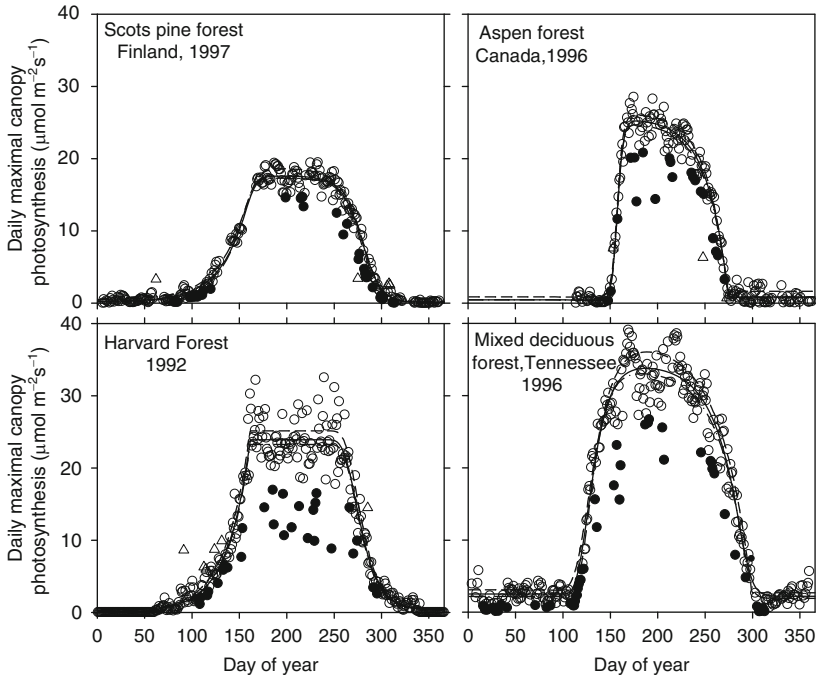
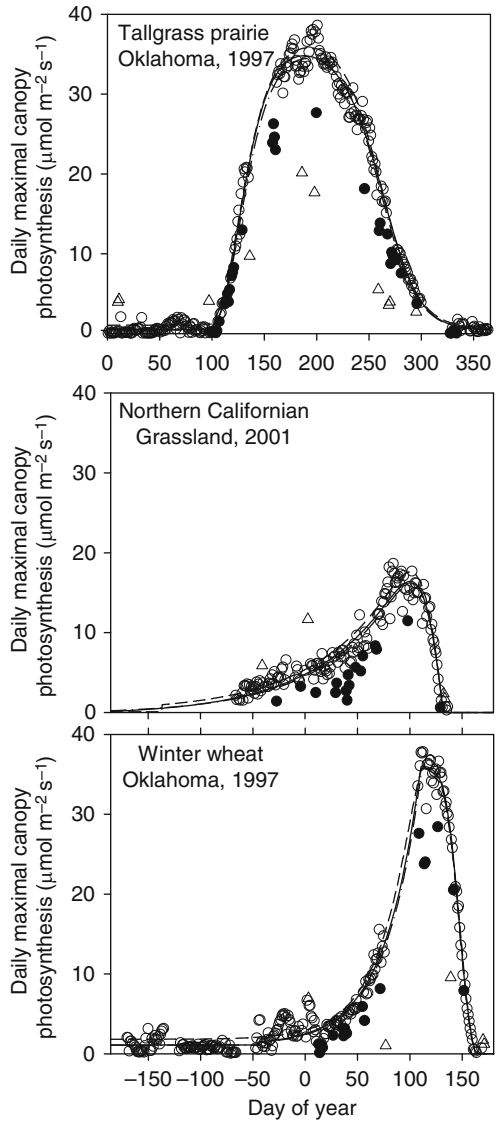


**Fig. 1** Seasonal variations of the daily maximal canopy photosynthetic rate for the four forest sites used in this study. *Triangles* denote outliers identified with the Grubb's test. Dots are data points whose corresponding ratios are at least one-standard deviation ( $1\sigma$ ) less than the mean ratio. The ratio here refers to the daily maximal canopy photosynthetic rate divided by a value predicted by Eqn. (1) for a given day. The prediction uses parameters obtained through fitting Eqn. (1) to the data that have survived the Grubb's test. The data that have passed both the Grubb's test and the  $1\sigma$  screening process are considered as the canopy photosynthetic capacity (CPC) and denoted by open circles. The solid line is the regression line of the final fitting of Eqn. (1) to the values of canopy photosynthetic capacity. For comparison, the final regression lines with two different standard deviation criteria ( $0\sigma$  and  $2\sigma$ ) are also shown. These lines are close to each other, indicating that the fitting is insensitive to the choice of filtering criteria.

photosynthetic rate to the predicted CPC. We remove the points with the ratio at least  $1\sigma$  less than the mean ratio (Step g). The choice of the  $1\sigma$  criterion is based on experiments with varying criteria to screening data affected by short-term weather conditions. Figures 1 and 2 show the fitted curves with different criteria ( $0\sigma$ ,  $1\sigma$ , and  $2\sigma$ ). Overall, these different criteria have only minor influence on the fitted curves. The curves with the  $1\sigma$  and  $2\sigma$  criteria are very close to each other. However, the fitted curves with the  $0\sigma$  criterion deviate relatively more from those with the  $1\sigma$  or  $2\sigma$  criteria, indicating that the  $0\sigma$  criterion may result in too few data to be used to represent the seasonal cycle of plant community photosynthesis and the fitted seasonal patterns with this more restrictive criterion may not be reliable. Therefore, we consider the  $1\sigma$  criterion as a balanced trade-off between the opposing

**Fig. 2** Same as Fig. 1, except for the tallgrass prairie site and the two cool-season vegetation sites (Californian grassland and winter wheat).



requirements of minimizing the influence of short-term weather variations vs. having a dataset with a sufficient number of samples for a robust fitting of the seasonal pattern.

The fitting for the parameters in Eqn. (1) is done with an optimization package developed as part of the AmeriFlux Data Assimilation Project at the Oak Ridge National Laboratory. Although describing this optimization package is beyond the

scope of current study, the quality of fitting shown in Figs. 1 and 2 attests to not only the suitability of Eqn. (1) for quantifying the seasonal dynamics of plant community photosynthesis but also the effectiveness of the optimization package. We have automated the procedures outlined above and the calculations of indices that characterize the seasonal dynamics of plant community photosynthesis.

## 4 Indices Characterizing the Seasonal Dynamics of Plant Community Photosynthesis

Indices that characterize the seasonal dynamics of plant community photosynthesis facilitate the comparison of different vegetation types across climate zones and the same vegetation in different years for functional disparities and similarities. These indices can also be related directly to environmental variables to reveal how changes in climate conditions affect the carbon assimilation of plant community. Using Eqn. (1), we have revised the set of indices proposed in Gu et al. (2003a) to provide a comprehensive terminological system for quantifying various features in the seasonal dynamics of plant community photosynthesis. A collection of these indices and their definitions is given in the appendix.

### 4.1 Characterizing the Dynamics in CPC

The growth rate ( $k$ ) of the CPC is the derivative of the canopy photosynthetic capacity with respect to the day ( $t$ ) of year:

$$k(t) = \frac{dA(t)}{dt} = \frac{a_1 c_1}{b_1} \frac{\exp\left(-\frac{t-t_{01}}{b_{01}}\right)}{\left[1 + \exp\left(-\frac{t-t_{01}}{b_{01}}\right)\right]^{1+c_1}} - \frac{a_2 c_2}{b_2} \frac{\exp\left(-\frac{t-t_{02}}{b_{02}}\right)}{\left[1 + \exp\left(-\frac{t-t_{02}}{b_{02}}\right)\right]^{1+c_2}} \quad (2)$$

The temporal dynamics in the growth rate  $k(t)$  of canopy photosynthetic capacity is interesting. Figures 3 and 4 show  $k(t)$  for the seven eddy covariance flux sites under this study. All seven sites, which include both warm-season and cool-season types, have one maximum and one minimum in  $k(t)$  over the growing season; the maximum occurs early and the minimum late in the growing season. The maximal growth rate of canopy photosynthetic capacity is termed “Peak Recovery Rate” and denoted by  $k_{PRR}$ ; the day on which this rate occurs is termed “Peak Recovery Day” and denoted by  $t_{PRD}$ :

$$k_{PRR} = k(t_{PRD}) \quad (3)$$

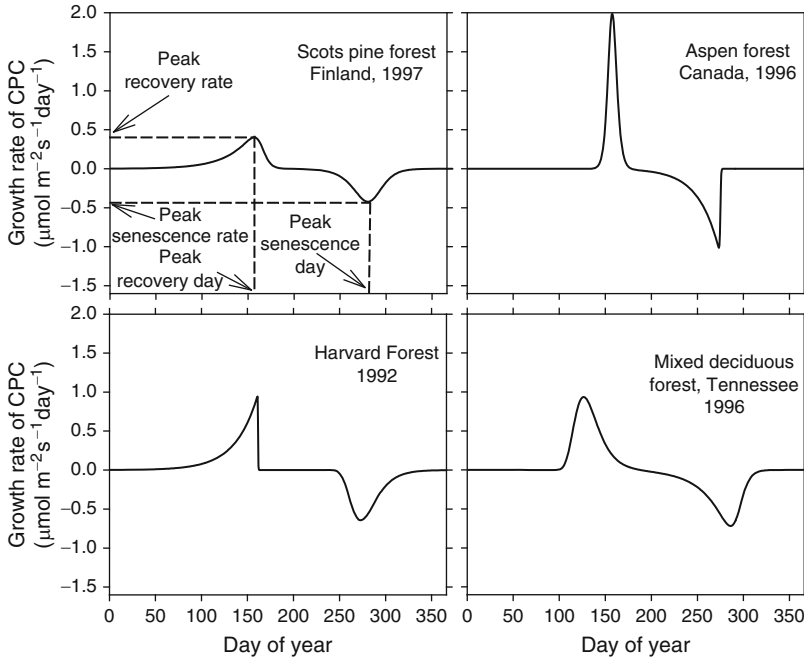


**Fig. 3** Temporal variations of the growth rate of canopy photosynthetic capacity (CPC) at the four forest sites.

We further define “Recovery Line” (RL) as the line that passes through the maximum with a slope of  $k_{PRR}$ . Its equation can be written as follows:

$$A_{RL}(t) = k_{PRR}t + A(t_{PRD}) - k_{PRR}t_{PRD} \tag{4}$$

where  $A_{RL}$  is the canopy photosynthetic capacity predicted by the Recovery Line. Similarly, we term the most negative growth rate of canopy photosynthetic capacity “Peak Senescence Rate” and denote it by  $k_{PSR}$  and the day on which  $k_{PSR}$  occurs “Peak Senescence Day” and denote it by  $t_{PSD}$ :

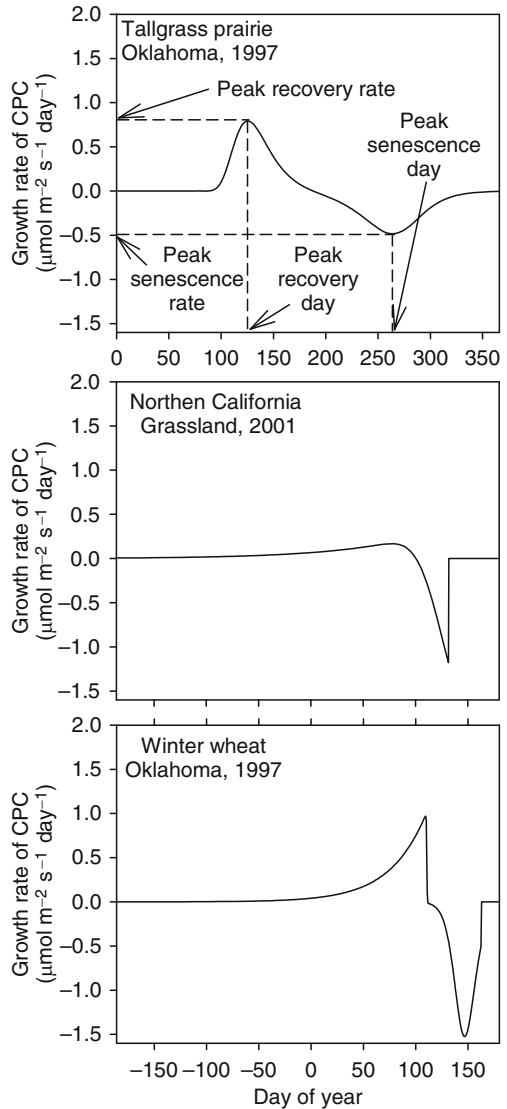
$$k_{PSR} = k(t_{PSD}) \tag{5}$$

Accordingly, we define “Senescence Line” (SL) as the line that passes through the minimum (the most negative) with a slope of  $k_{PSR}$  and describe it by the following equation:

$$A_{SL}(t) = k_{PSR}t + A(t_{PSD}) - k_{PSR}t_{PSD} \tag{6}$$

where  $A_{SL}$  is the canopy photosynthetic capacity predicted by the Senescence Line.

**Fig. 4** Temporal variations of the growth rate of canopy photosynthetic canopy (CPC) at the tallgrass prairie site and the two cool-season sites (Californian grassland and winter wheat).



It is very difficult to determine  $t_{PRD}$  and  $t_{PSD}$  analytically from Eqn. (1). However, they can be approximated by:

$$t_{PRD} \approx t_{01} + b_1 \ln(c_1) \quad (7)$$

and

$$t_{PSD} \approx t_{02} + b_2 \ln(c_2) \quad (8)$$

Equation (7) is obtained by setting the derivative of the first term in Eqn. (2) with respect to  $t$  to zero and solve for  $t$  where the first term is at maximum; Eqn. (8) is obtained by setting the derivative of the second term in Eqn. (2) with respect to  $t$  to zero and solve for  $t$  where the second term is at maximum. Equations (7) and (8) hold because when  $t$  is small, the second term in Eqn. (2) is close to zero and when  $t$  is large, the first term is close to zero. Alternatively, one could simply compute the value of  $k$  for each day of the year and pick up the maximum and the minimum as we did in this study.

The RL and SL defined through the maximum and minimum in the growth rate of canopy photosynthetic capacity capture the two linear features in the temporal variation of canopy photosynthetic capacity very well (Figs. 5 and 6). These two linear features occupy two crucial periods of time in the growing season and dominate the overall shape of the seasonal cycle and thus are important for studying plant community photosynthesis. In Gu et al. (2003a), these linear features are fit with the lines determined by the minima in the radius of curvature. While the minimum in the radius of curvature is a clear mathematical concept, it has no ecological

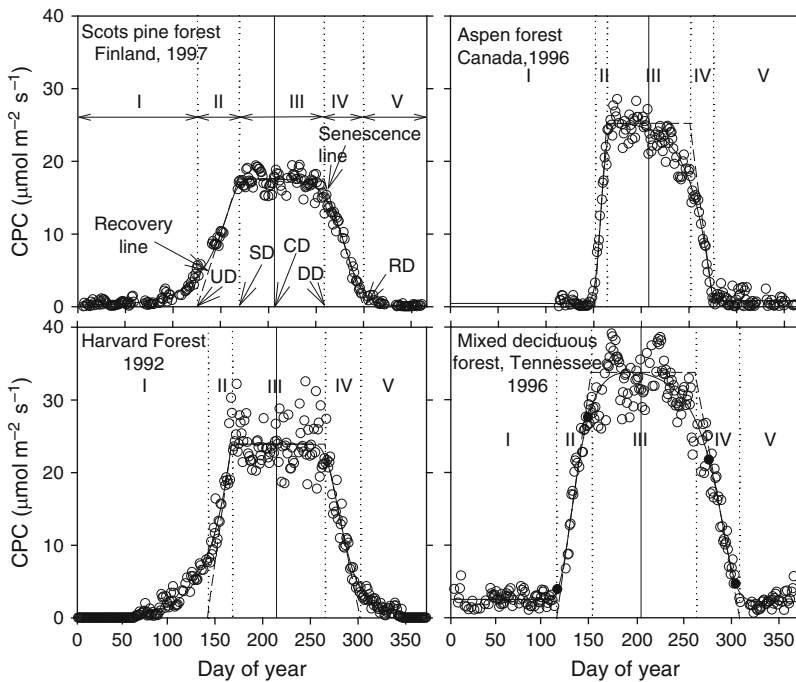
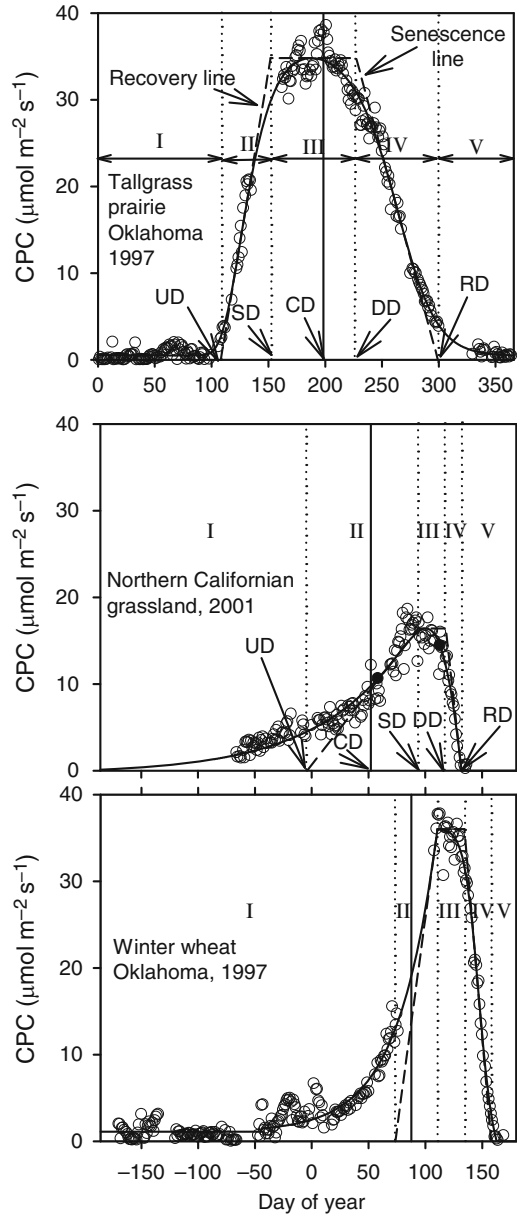


**Fig. 5** Temporal variations of canopy photosynthetic capacity (CPC) for the four forest sites. Marked are the five phases of photosynthetic dynamics, upturn day (UD), stabilization day (SD), center day (CD), downturn day (DD), recession day (RD), the recovery line, and the senescence line. The line that parallels the x-axis and links the recovery and senescence lines indicates peak canopy photosynthetic capacity.

**Fig. 6** Same as Fig. 5, except for the tallgrass prairie site and the two cool-season vegetation sites (Californian grassland and winter wheat).



correspondence and thus it is difficult to relate it with any underlying biological or environmental processes. In contrast, it is easy to interpret the ecological meaning of the maximum (minimum) in the growth rate of canopy photosynthetic capacity. Thus the new way of defining the recovery and senescence linear features in  $A(t)$  is more desirable.

## 4.2 Characterizing Canopy Photosynthetic Potential

The area under the curve of  $A(t)$  is an indicator of how much carbon dioxide can be potentially assimilated by a plant community over a complete cycle of photosynthesis in a year. Although the actual amount of carbon dioxide assimilated is also influenced by the diurnal cycle and variation in short-term weather conditions, a plant community that maximizes this area can fully realize the potential of carbon dioxide assimilation allowable by variation in climatic conditions in a year. As in Gu et al. (2003a), we term this area “Carbon Assimilation Potential” ( $u$ ):

$$u = \int_{t_{\text{start}}}^{t_{\text{end}}} A(t) dt \quad (9)$$

In theory, the above integration could start from the beginning to the end of the growing season, e.g., the start day  $t_{\text{start}}$  and the end day  $t_{\text{end}}$  could be set as the first and last day, respectively, for the period of time when the canopy photosynthetic capacity  $A > 0$ . In practice, it is very difficult to determine these two dates exactly from data as  $A$  changes very gradually at the beginning and end of the growing season. However, for the purpose of calculating the carbon assimilation potential  $u$ , it is not necessary to determine  $t_{\text{start}}$  and  $t_{\text{end}}$  exactly as long as one whole seasonal cycle of photosynthesis is included between  $t_{\text{start}}$  and  $t_{\text{end}}$ . This is because the two tails of  $A$  contribute little to  $u$ . Therefore we conveniently set  $t_{\text{start}} = 1$  and  $t_{\text{end}} = 365$  for warm-season vegetation sites (Figs. 5 and 6a) and  $t_{\text{start}} = -185$  and  $t_{\text{end}} = 180$  for cool-season vegetation sites (June–June, Fig. 6b, c). Clearly, here we don’t intend to use  $t_{\text{start}}$  ( $t_{\text{end}}$ ) to denote the start (end) of the growing season.

The peak canopy photosynthetic capacity over a complete seasonal cycle of plant community photosynthesis and the day on which this peak occurs should contain useful information about the function of the vegetation and its interaction with the climate. We use  $A_p$  to denote the peak canopy photosynthetic capacity:

$$A_p = \max \left\{ A(t), t_{\text{start}} < t < t_{\text{end}} \right\} \quad (10)$$

We use  $t_p$  to denote the day on which the peak canopy photosynthetic capacity occurs.  $t_p$  is called “Peak Canopy Photosynthetic Capacity Day” or simply “Peak Capacity Day.”

## 4.3 The Five Phases of the Seasonal Cycle of Plant Community Photosynthesis

As shown in Figs. 5 and 6, the seasonal cycle of plant community photosynthesis can be divided into five consecutive phases:

- Phase I.* Pre-phase, a slowly crawling-up stage at the beginning of the growing season.
- Phase II.* Recovery phase, a rapid recovery and expansion period.

*Phase III.* Stable phase, a relatively steady stage in the middle of the growing season.

*Phase IV.* Senescence phase, a rapidly declining stage after the stable phase.

*Phase V.* Termination phase, a fading stage towards the end of the growing season.

Although different vegetation types may show different characteristics in their seasonal cycles of photosynthesis, the similarity among them is also striking. Throughout a year, plant canopies undergo systematic changes in anatomy, biochemistry and physiology; understanding how these systematic changes interact with seasonal marches in climatic conditions to determine canopy carbon fixation is vital to understanding the functioning of plant communities and the terrestrial carbon cycle. For example, in deciduous canopies, both leaf area index (LAI) and leaf photosynthetic capacities increase in spring and remain relatively stable in the middle of the growing season and then decrease in fall (Wilson et al. 2000; Hikosaka 2003; Niinemets et al. 2004). Many understory plant species take advantage of the high light period prior to canopy closure in early spring or after leaf fall in autumn to fix carbon dioxide and accumulate carbohydrates to prepare for new growth (Routhier and Lapointe 2002; Richardson and O'Keefe, current volume). These biological and ecological processes produce both transient and steady features in the seasonal dynamics of plant community photosynthesis. Understanding processes operating in and factors controlling the transition between different phases of plant community photosynthesis should be an interesting research task for plant ecologists.

#### 4.4 Transitions Between Phases

We name the transitions between the consecutive phases identified above “Upturn Day” ( $t_U$ ), “Stabilization Day” ( $t_S$ ), “Downturn Day” ( $t_D$ ), and “Recession Day” ( $t_R$ ), respectively. We set the upturn day at the intersection between the recovery line and the  $x$ -axis and the recession day at the intersection between the senescence line and the  $x$ -axis. The upturn day and recession day are calculated from Eqns. (4) and (6), respectively, as follows:

$$t_U = t_{PRD} - A \frac{t_{PRD}}{k_{PRR}} \quad (11)$$

$$t_R = t_{PSD} - A \frac{t_{PSD}}{k_{PSR}} \quad (12)$$

The stabilization day and downturn day are set at the days on which the peak canopy photosynthetic capacity  $A_p$  is predicted to occur based on the RL equation (4) and the SL equation (6), respectively. These two dates are given by:

$$t_S = t_{PRD} + \frac{(A_p - A t_{PRD})}{k_{PRR}} \quad (13)$$

$$t_D = t_{PSD} + \frac{(A_P - At_{PSD})}{k_{PSR}} \quad (14)$$

Note that in the present paper the terms of upturn day, stabilization day, downturn day, and recession day are used somewhat differently from those in Gu et al. (2003a). They were the names for the four minima in the radius of curvature of  $A(t)$  in that previous paper. The four turning points defined by RL and SL have similar meanings as intended in Gu et al. (2003a). Therefore, we continue to use the same terms in the present paper.

#### 4.5 Effective Growing Season Length

Although it is very difficult to determine unequivocally dates for the start and end of the growing season, the upturn day and recession day come close, particularly for the five sites where plants grow in the summer (Figs. 5 and 6a). For these warm-season vegetation sites, the area under the curve of  $A(t)$  between  $t_U$  and  $t_R$  accounts for more than 90% of the corresponding canopy carbon assimilation potential  $u$  (97% in tallgrass prairie, 94% in Scots pine and aspen forests, 92% in Harvard Forest and the mixed forest in Tennessee, 83% in California grassland and 75% in winter wheat). Therefore,  $t_U$  and  $t_R$  may be used to approximate the start and end, respectively, of the growing season for the warm-season vegetation type. However, there is still substantial photosynthesis (~20%) outside the period between  $t_U$  and  $t_R$  for the cool-season vegetation type. Consequently, for these sites,  $t_U$  and  $t_R$  are not good markers for the growing season; nevertheless, they can be used to indicate the “active period” of the growing season. Similar functions can be played by the peak recovery and senescence days which can be used to mark the period of the growing season during which the photosynthetic activity of the plant community is strong.

We can also use the standard deviation of the “growing days” to measure the length of the growing season. To do so, we first define the mean or Center Day ( $t_C$ ) of the growing season as follows:

$$t_C = \frac{\int_{t_{start}}^{t_{end}} tA(t)dt}{u} \quad (15)$$

The standard deviation  $\sigma$  of the “growing days” from the center day of the growing season is:

$$\sigma = \left( \frac{\int_{t_{start}}^{t_{end}} (t - t_C)^2 A(t)dt}{u} \right)^{0.5} \quad (16)$$

The length of the growing season can then be measured by the scaled standard deviation:

$$L_E = 2\sqrt{3}\sigma \quad (17)$$

We name the scaled standard deviation the “Effective Growing Season Length” and denote it by  $L_E$ . The scaling factor  $2\sqrt{3}\sigma$  is introduced so that  $L_E$  is exactly the width if the temporal pattern of  $A(t)$  is a rectangle (Gu et al. 2003a). Gu et al. (2003a) defined the center day as the “center of gravity” of the curve  $A(t)$ . In the present paper, the center day is defined as a statistical mean and is thus more straightforward.

#### 4.6 Effective Canopy Photosynthetic Capacity

From the carbon assimilation potential index and the effective growing season length, we can then define the seasonal “Effective Canopy Photosynthetic Capacity” ( $A_E$ ) as:

$$A_E = \frac{u}{L_E} \quad (18)$$

#### 4.7 Shape Parameters of the Seasonal Patterns of Plant Community Photosynthesis

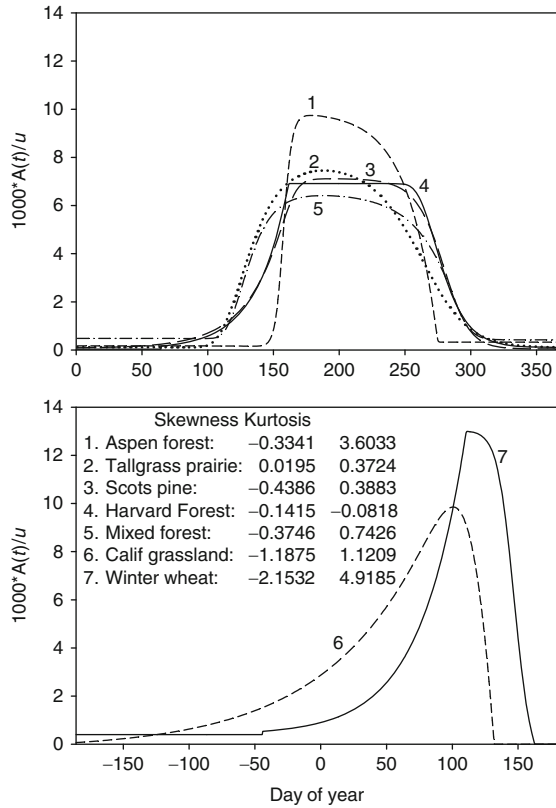
The shape of the seasonal cycle of plant community photosynthesis often differs greatly among different sites. Borrowing two shape parameters from statistics, we define the Skewness ( $\gamma_S$ ) and Kurtosis ( $\gamma_K$ ) of the seasonal pattern of plant community photosynthesis as follows:

$$\gamma_S = \frac{1}{u} \int_{t_{start}}^{t_{end}} \left( \frac{t - t_C}{\sigma} \right)^3 A(t) dt \quad (19)$$

$$\gamma_K = \frac{1}{u} \int_{t_{start}}^{t_{end}} \left( \frac{t - t_C}{\sigma} \right)^4 A(t) dt - 3 \quad (20)$$

Figure 7 shows the temporal variation of the canopy photosynthetic capacity scaled by the carbon assimilation potential (i.e.  $A/u$ ) with the values of skewness and kurtosis marked for the seven vegetation sites (the scaling makes the comparison among different curves easier). The skewness parameter is more negative if the photosynthetic activities are skewed to the end of the growing season (e.g. the cool-season vegetations, Fig. 7b). The kurtosis parameter is larger if the peak of the seasonal photosynthesis is sharper (e.g. the aspen forest vs. other warm-season vegetations, Fig. 7a). Different skewness and kurtosis may reflect adaptations of plant communities to specific climate conditions.

**Fig. 7** The canopy photosynthetic capacity scaled for comparison in the shape of temporal variation among different sites.



## 5 Application for Synthesis Across Sites

How useful is the framework described above? To answer this question, we need to examine how general the concepts and method of analysis developed are and more importantly, whether their application can lead to new scientific findings, questions, and testable hypotheses. Although the number of sites included in this study is limited (seven in total), the broad range of vegetation types covered indicates that the framework we developed can be widely applied. In the following, two synthesis examples are used to demonstrate that analyzing the dynamics of plant community photosynthesis based on the developed framework can produce fruitful scientific results. Table 1 summarizes the indices of photosynthetic cycles calculated for the seven vegetation sites in this study.

**Table 1** Values of indices characterizing the dynamics of plant community photosynthesis at the seasonal time scale for the seven vegetation sites involved in this study. Study site abbreviations: *SP* scots pine, *AF* aspen forest, *HF* Harvard Forest, *TM* Tennessee mixed forest, *TP* tallgrass prairie, *CG* California grassland, *WW* winter wheat. Units of indices are given in the Appendix

Index	<i>SP</i>	<i>AF</i>	<i>HF</i>	<i>TM</i>	<i>TP</i>	<i>CG</i>	<i>WW</i>
Peak recovery rate	0.40	1.99	0.95	0.94	0.79	0.17	0.97
Peak recovery day	157	158	161	127	126	77	110
Peak senescence rate	-0.42	-1.02	-0.65	-0.72	-0.48	-1.20	-1.52
Peak senescence day	280	273	273	286	264	132	147
Carbon assimilation potential	2,473	2,589	3,460	5,267	4,671	1,666	2,773
Peak canopy photosynthetic capacity	17.58	25.23	23.91	33.76	34.80	16.41	36.03
Peak capacity day	193	178	193	188	188	101	112
Effective canopy photosynthetic capacity	14.40	17.72	20.73	25.53	27.60	8.12	12.65
Upturn day	125	151	136	111	108	361	73
Stabilization day	169	164	162	147	152	94	111
Downturn day	258	251	260	256	227	118	134
Recession day	300	276	297	303	299	132	158
Center day	206	208	209	200	199	52	88
Effective growing season length	172	146	167	206	169	205	219
Skewness	-0.44	-0.33	-0.14	-0.37	0.02	-1.19	-2.15
Kurtosis	0.39	3.60	-0.08	0.74	0.37	1.12	4.92

## 5.1 The Recovery–Senescence Relationship

The first synthesis example we present here is the relationship between the peak recovery rate and the peak senescence rate across sites (Fig. 8). For warm-season vegetation sites, the peak recovery rates are generally larger than the peak senescence rates. For cool-season vegetation sites, the opposite is true. But more interestingly, the relationship between the peak recovery and senescence rates seems linear across the warm-season vegetation sites. This close relationship between community photosynthetic recovery and senescence is unlikely due to the fitting function of choice since the function fits the data tightly, particularly for the linear features in the temporal variation of the canopy photosynthetic capacity (Figs. 5 and 6) and since a linear relationship was also reported by Gu et al. (2003a) who used a different fitting function. Therefore, the recovery–senescence linear relationship likely reflects a true conservative characteristic of plant community photosynthesis across sites. It may imply that the efficiency of a warm-season plant community to mobilize resources (nutrients and carbohydrates) to develop photosynthetic machinery in response to rapidly improving atmospheric conditions at the start of the growing season is closely related to its efficiency to withdraw and preserve crucial resources from leaves before abscission in response to deteriorating environmental conditions near the end of the growing season.

We have too few cool-season sites (only two) and thus cannot draw any firm conclusion regarding the recovery–senescence relationship for the cool-season vegetation

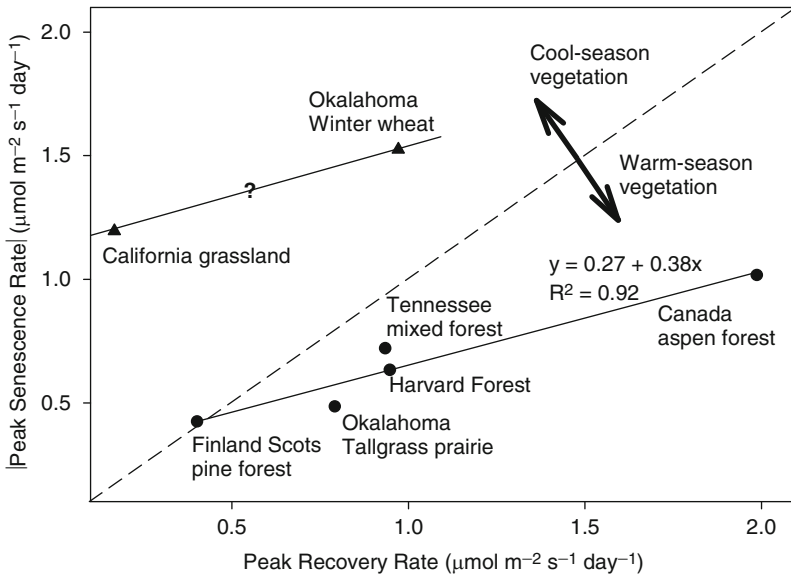


**Fig. 8** The relationship between peak recovery and senescence rates across sites. The absolute values of peak senescence rates are used.

type. But this does not preclude us from pointing out the following observation: the line that passes through the two cool-season sites in the figure of peak recovery vs. senescence rate parallels the regression line for the warm-season vegetation type (Fig. 8). The probability that these two lines parallel each other by chance must be very low, considering that the sites involved were geographically separated and measurements used to derive these lines were independently acquired. If it is not due to chance, then there are grounds for making the following two hypotheses:

1. The relationship between the recovery and senescence of plant community photosynthesis is linear for the cool-season vegetation type as it is for the warm-season vegetation type.
2. The recovery-senescence relationship is invariant between the warm-season and cool season vegetation types, up to an offset in the intercept.

## 5.2 Factors Affecting the Carbon Assimilation Potential

The second example of using the developed methodology for synthesis across sites concerns the factors affecting the carbon assimilation potential. As we pointed out earlier, the carbon assimilation potential is an important measure of how much carbon dioxide can be assimilated in a year by a plant community under the constraint of climate. The carbon assimilation potential can be maximized by increasing the peak canopy photosynthetic capacity and/or the growing season length.

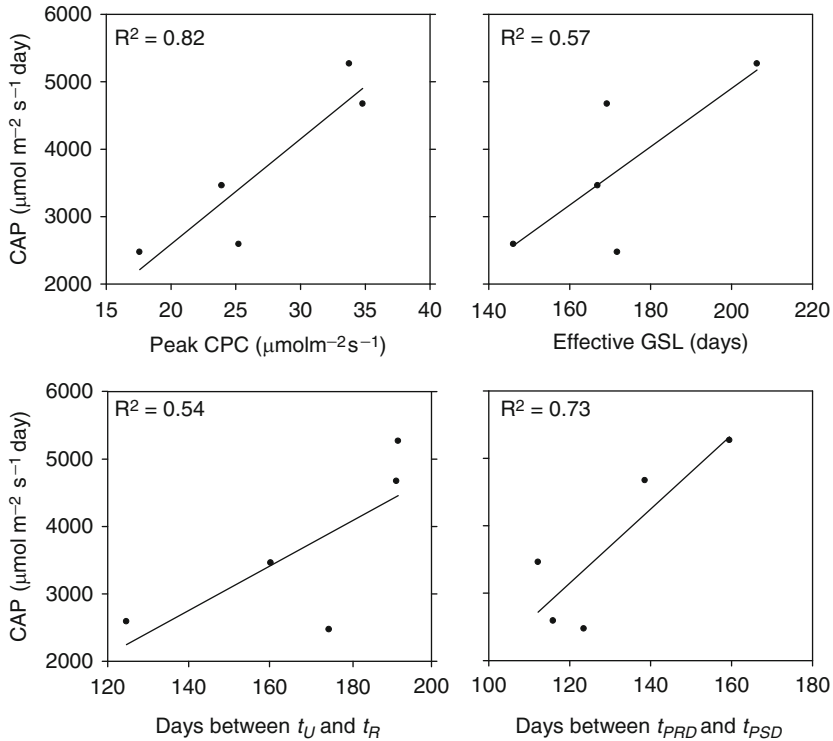


**Fig. 9** The change of the carbon assimilation potential (CAP) with the peak canopy photosynthetic capacity (CPC) and with different measures of the growing season length (GSL).  $t_U$ , Upturn Day;  $t_R$ , Recession Day;  $t_{PRD}$ , Peak Recovery Day;  $t_{PSD}$ , Peak Senescence Day. Only the warm-season vegetation sites are included.

Figure 9 compares, for the warm-season vegetation type, the relationship between the carbon assimilation potential and the peak canopy photosynthetic capacity with various measures of the growing season length. For this synthesis, the cool-season vegetation type is not included because the number of cool-season sites is too few and because the control for the carbon assimilation potential is obviously different between the warm and cool-season vegetation types. The comparison shown in Fig. 9 indicates the peak canopy photosynthetic capacity is a better predictor for the canopy carbon assimilation potential than are the measures of the growing season length. Although common ecological and environmental factors affect both peak canopy photosynthetic capacity and growing season length, different factors have variable degrees of influence on them. Peak canopy photosynthetic capacity should be strongly affected by leaf photosynthetic capacity and leaf area index of the canopy (Noormets et al., current volume). Leaf photosynthetic capacity and leaf area index are controlled primarily by nutrient and water availability at a site. In contrast, growing season length is determined mainly by climate conditions (i.e. temperature, photoperiod, etc). Thus the finding that peak canopy photosynthetic capacity is a better predictor of carbon assimilation potential than are measures of

growing season length may indicate that ecophysiological conditions such as nutrient and water availability could be more important than the variation in climate conditions in controlling carbon dioxide assimilation at the seasonal time scale.

## 6 Discussion and Conclusions

In this chapter we continued the effort initiated in Gu et al. (2003a) to develop the methodology for analyzing the dynamics of plant community photosynthesis at the seasonal time scale based on eddy covariance flux measurements. We proposed a new function to represent the photosynthetic cycle of plant communities and suggested that the dynamics of plant community photosynthesis generally consist of five distinctive phases in sequence. These phases are pre-phase, recovery phase, stable phase, senescence phase, and termination phase; each phase results from the interactions between the inherent biological and ecological processes and the progression of climatic conditions and reflects unique functioning of plant communities at different stages of the growing season. We also improved the set of indices to characterize and quantify the transitions between phenophases in the dynamics of plant community photosynthesis.

We applied the improved framework of analysis to seven vegetation sites which ranged from evergreen and deciduous forests to crop to grasslands and include both cool-season and warm-season vegetation types. We found that for the warm-season vegetation type, the recovery of plant community photosynthesis at the beginning of the growing season was faster than the senescence at the end of the growing season while for the cool-season vegetation type, the opposite was true. Additionally, for the warm-season vegetation type, the recovery was closely correlated with the senescence such that a faster photosynthetic recovery was associated with speedier photosynthetic senescence and *vice versa*. We hypothesized that a similar close correlation could also exist for the cool-season vegetation type, and furthermore, the recovery–senescence relationship may be invariant between the warm-season and cool-season vegetation types up to an offset in the intercept. This hypothesis, which the present analysis aroused but didn't have enough data to confirm, awaits more studies. We also found that while the growing season length affected how much carbon dioxide could be potentially assimilated by a plant community over the course of a growing season, ecophysiological factors that affect leaf area/photosynthetic capacity development (e.g. nutrient and water availability) could be even more important at this scale. This implies that the climate warming-induced increase in the growing season length may have a limited enhancement effect on the terrestrial carbon uptake. These results and insights demonstrate that the proposed method of analysis and system of terminology can serve as a foundation for studying the dynamics of plant community photosynthesis and such studies can be fruitful.

Where should we go from here? The dynamics of plant community photosynthesis need to be studied at more eddy covariance flux sites, especially, Mediterranean or cool-season vegetation sites. A greatly expanded analysis would allow us to develop a comprehensive picture on how the photosynthetic phenological indices of plant

community as well as the relationships among them change with vegetation types and climatic conditions. Cross-site emergent patterns such as the conserved relationship between peak recovery rate and peak senescence rate (Fig. 8) and the dominant control of carbon assimilation potential by peak canopy photosynthetic capacity (Fig. 9) could be confirmed or established. Mechanistic explanations of these emergent patterns may require development of new ecological theories and in-depth physiological and biochemical studies of underlying processes. These efforts could serve as the starting point for developing the science of community photosynthesis. Within this new scientific discipline, many outstanding questions could be pursued. For example, do different plant communities have their unique photosynthetic signatures? How do changes in climate and soil nutrient conditions drive photosynthetic cycle events? How are photosynthetic cycle events related to vegetation structural cycle events? Understanding of molecular and leaf photosynthesis will be necessary but not sufficient for developing answers to these questions just as the advantage of diffuse radiation at the canopy level cannot be explained based on molecular and leaf photosynthesis alone (Gu et al. 2002, 2003b). We will need to study how the characteristics of plant community photosynthesis are related to traits and adaptations of individual species in the community, how plant community as a whole shapes its photosynthetic adaptation and evolution under environmental changes, and how plant community photosynthetic cycles interact with soil nutrient and carbon pool dynamics. In particular, fruitful results could be obtained by investigating the recovery–senescence relationship and its physiological basis.

**Acknowledgements** We thank Drs. Rich Norby and Asko Noormets for commenting on the paper. This study was supported by the U.S. Department of Energy, Office of Science, Biological and Environmental Research Program, Environmental Science Division. Oak Ridge National Laboratory (ORNL) is managed by UT-Battelle, LLC, for the U.S. Department of Energy under the contract DE-AC05-00OR22725.

## Appendix: List of Terms

*Canopy photosynthetic capacity* ( $A$ ,  $\mu\text{mol m}^{-2} \text{s}^{-1}$ ): the maximal gross photosynthetic rate at the canopy level that can be expected for a plant community at a given time of a year when the seasonal variation in climatic conditions is taken into account.

*Carbon assimilation potential* ( $u$ ,  $\mu\text{mol m}^{-2} \text{s}^{-1} \text{ day}$ ): the integration of canopy photosynthetic capacity over a year (the area under the curve of canopy photosynthetic capacity in a plot of canopy photosynthetic capacity vs. day of year).

*Center day* ( $t_c$ , the number of days from 1<sup>st</sup> Jan.): the mean “growing day  $t$  of year” when  $t$  is treated as a random variable whose “probability density function” is  $A(t)/u$  where  $A$  is the canopy photosynthetic capacity and  $u$  the carbon assimilation potential.

*Downturn day* ( $t_d$ , the number of days from 1<sup>st</sup> Jan.): the day on which the peak canopy photosynthetic capacity is predicted to occur based on the senescence line. Around the downturn day, canopy photosynthetic capacity often starts to decrease sharply.

*Effective canopy photosynthetic capacity* ( $A_E$ ,  $\mu\text{mol m}^{-2} \text{s}^{-1}$ ): the ratio of the carbon assimilation potential to the effective growing season length.

*Effective growing season length* ( $L_E$ , days): the scaled standard deviation of the “growing day  $t$  of year” when  $t$  is treated as a random variable whose probability density function is  $A(t)/u$  where  $A$  is the canopy photosynthetic capacity and  $u$  the carbon assimilation potential.

- Kurtosis* ( $\gamma_K$ ): a measure of the peakedness of the curve  $A(t)$ , the scaled and shifted fourth central moment of the “probability density function”  $A(t)/u$ .
- Peak capacity day* ( $t_p$ , the number of days from 1<sup>st</sup> Jan): the day on which the peak canopy photosynthetic capacity and thus the peak of the growing season occur.
- Peak canopy photosynthetic capacity* ( $A_p$ ,  $\mu\text{mol m}^{-2} \text{s}^{-1}$ ): the peak of the canopy photosynthetic capacity during the growing season.
- Peak recovery day* ( $t_{PRD}$ , the number of days from 1<sup>st</sup> Jan.): the day of the year on which the peak recovery rate occurs.
- Peak recovery rate* ( $k_{PRR}$ ,  $\mu\text{mol m}^{-2} \text{s}^{-1} \text{ day}^{-1}$ ): the largest growth rate of canopy photosynthetic capacity during the growing season.
- Peak senescence day* ( $t_{PSD}$ , the number of days from 1<sup>st</sup> Jan.): the day of the year on which the peak senescence rate occurs.
- Peak senescence rate* ( $k_{PSR}$ ,  $\mu\text{mol m}^{-2} \text{s}^{-1} \text{ day}^{-1}$ ): the most negative growth rate of canopy photosynthetic capacity during the growing season.
- Pre-phase* (Phase I): the initial stage of the seasonal cycle of plant community photosynthesis during which canopy photosynthetic capacity tends to increase slowly and often steadily.
- Recession day* ( $t_R$ , the number of days from 1<sup>st</sup> Jan): the day on which the senescence line intercepts with the  $x$ -axis.
- Recovery line* (RL): a line that closely approximates the linear feature within the recovery phase (Phase II) of the seasonal dynamics of plant community photosynthesis and is defined by the canopy photosynthetic capacity and its growth rate on the peak recovery day.
- Recovery phase* (Phase II): the second stage of the seasonal cycle of plant community photosynthesis during which the canopy photosynthetic capacity tends to increase rapidly and linearly.
- Senescence line* (SL): a line that closely approximates the linear feature during the senescence phase (Phase IV) of the seasonal dynamics of plant community photosynthesis and is defined by the canopy photosynthetic capacity and its growth (decline) rate (negative) on the peak senescence day.
- Senescence phase* (Phase IV): the fourth stage of the seasonal cycle of plant community photosynthesis during which canopy photosynthetic capacity tends to decline rapidly and linearly.
- Skewness* ( $\gamma_S$ ): a measure of the asymmetry of the curve  $A(t)$ , the scaled third central moment of the ‘probability density function’  $A(t)/u$ .
- Stabilization day* ( $t_s$ , the number of days from 1<sup>st</sup> Jan): the day on which the peak canopy photosynthetic capacity is predicted to occur based on the recovery line.
- Stable phase* (Phase III): the third stage of the seasonal cycle of plant community photosynthesis during which canopy photosynthetic capacity remains relatively stable.
- Termination phase* (Phase V): the final stage of the seasonal cycle of plant community photosynthesis during which canopy photosynthetic capacity is reduced to zero or approaches to zero slowly.
- Upturn day* ( $t_u$ , the number of days from 1<sup>st</sup> Jan.): the day on which the recovery line intercepts with the  $x$ -axis. Around the upturn day, the canopy photosynthetic capacity often starts to increase sharply.

## References

- Baldocchi DD, Falge E, Gu LH, Olson R, Hollinger D, Running S, Anthoni P, Bernhofer C, Davis KJ, Evans R, Fuentes JD, Goldstein AH, Katul G, Law BE, Lee X, Malhi Y, Meyers T, Munger W, Oechel W, Paw U KT, Pilegaard K, Schmid HP, Valentini R, Verma S, Vesala T, Wilson K, Wofsy S. 2001. FLUXNET: A new tool to study the temporal and spatial variability of ecosystem-scale carbon dioxide, water vapor, and energy flux densities. *Bulletin of the American Meteorological Society* 82:2415–34.
- Baldocchi, D., Hicke, B.B. and Meyers, T.P. (1988) Measuring biosphere-atmosphere exchanges of biologically related gases with micrometeorological methods. *Ecology* 69, 1331–1340.
- Baldocchi, D.D. (2003) Assessing the eddy covariance technique for evaluating carbon dioxide exchange rates of ecosystems: past, present and future. *Global Change Biol.* 9, 479–492.

- Baldocchi, D.D., Xu, L.K. and Kiang, N. (2004) How plant functional-type, weather, seasonal drought, and soil physical properties alter water and energy fluxes of an oak–grass savanna and an annual grassland. *Agric. For. Meteorol.* 123, 13–39.
- Black, T.A., Chen, W.J., Barr, A.G., Arain, M.A., Chen, Z., Nesci, Z., Hogg, E.H., Neumann, H.H. and Yang, P.C. (2000) Increased carbon sequestration by a boreal deciduous forest in years with a warm spring. *Geophys. Res. Lett.* 27, 1271–1274.
- Bowling, D.R., Pieter, P.T. and Monson, R.K. (2001) Partitioning net ecosystem carbon exchange with isotopic fluxes of CO<sub>2</sub>. *Global Change Biol.* 7, 127–145.
- Burba, G.G. and Verma, S.B. (2005) Seasonal and interannual variability in evapotranspiration of native tallgrass prairie and cultivated wheat ecosystems. *Agric. For. Meteorol.* 135, 190–201.
- Campbell, J.E., Carmichael, G.R., Chai, T., Mena-Carrasco, M., Tang, Y., Blake, D.R., Blake, N.J., Vay, S.A., Collatz, G.J., Baker, I., Berry, J.A., Montzka, S.A., Sweeney, C., Schnoor, J.L. and Stanier, C.O. (2008) Photosynthetic control of atmospheric carbonyl sulfide during the growing season. *Science* 322, 1085–1088.
- Falge, E., Baldocchi, D.D., Tenhunen, J., Aubinet, M., Bakwin, P.S., Berbigier, P., Bernhofer, C., Burba, G., Clement, R., Davis, K.J., Elbers, J.A., Goldstein, A.H., Grelle, A., Granier, A., Guddmundsson, J., Hollinger, D., Kowalski, A.S., Katul, G., Law, B.E., Malhi, Y., Meyers, T., Monson, R.K., Munger, J.W., Oechel, W., Paw U, K.T., Pilegaard, K., Rannik, Ü., Rebmann, C., Suyker, A., Valentini, R., Wilson, K. and Wofsy, S. (2002) Seasonality of ecosystem respiration and gross primary production as derived from FLUXNET measurements. *Agric. For. Meteorol.* 113, 53–74.
- Goulden, M.L., Munger, J.W., Fan, S.M., Daube, B.C. and Wofsy, S.C. (1996) Measurements of carbon sequestration by long-term eddy covariance: methods and critical evaluation of accuracy. *Global Change Biol.* 2, 169–182.
- Gu, L. and Baldocchi, D.D. (2002) Foreword to the Fluxnet special issue. *Agric. For. Meteorol.* 113, 1–2.
- Gu, L., Post, W.M., Baldocchi, D., Black, T.A., Verma, S.B., Vesala, T. and Wofsy, S.C. (2003a). Phenology of vegetation photosynthesis. In: Schwartz, M.D. (Ed.) *Phenology: An Integrated Environmental Science*. Kluwer, Dordrecht, pp. 467–485.
- Gu, L.H., Baldocchi, D.D., Verma, S.B., Black, T.A., Vesala, T., Falge, E.M. and Dowty, P.R. (2002) Advantages of diffuse radiation for terrestrial ecosystem productivity. *J. Geophys. Res. (D Atmos.)* 107, art. no. 4050.
- Gu, L.H., Baldocchi, D.D., Wofsy, S.C., Munger, J.W., Michalsky, J.J., Urbanski, S.P. and Boden, T.A. (2003b) Response of a deciduous forest to the Mount Pinatubo eruption: Enhanced photosynthesis. *Science* 299, 2035–2038.
- Hikosaka, K. (2003) A model of dynamics of leaves and nitrogen in a plant canopy: An integration of canopy photosynthesis, leaf life span, and nitrogen use efficiency. *Am. Nat.* 162, 149–164.
- Liu, Q., Edwards, N.T., Post, W.M., Gu, L., Ledford, J. and Lenhart, S. (2006) Temperature-independent diel variation in soil respiration observed from a temperate deciduous forest. *Global Change Biol.* 12, 2136–2145.
- Niinemets, Ü., Kull, O. and Tenhunen, J.D. (2004) Within-canopy variation in the rate of development of photosynthetic capacity is proportional to integrated quantum flux density in temperate deciduous trees. *Plant Cell Environ.* 27, 293–313.
- NIST/SEMATECH (2006) e-Handbook of Statistical Methods. <http://www.itl.nist.gov/div898/handbook/>.
- Rannik, Ü., Aubinet, M., Kurbanmuradov, O., Sabelfeld, K.K., Markkanen, T. and Vesala, T. (2000) Footprint analysis for measurements over a heterogeneous forest. *Bound.-Lay. Meteorol.* 97, 137–166.
- Routhier, M.C. and Lapointe, L. (2002) Impact of tree leaf phenology on growth rates and reproduction in the spring flowering species *Trillium erectum* (Liliaceae). *Am. J. Bot.* 89, 500–505.
- Schwartz, M.D. (Ed.) (2003) *Phenology: An Integrative Environmental Science*. Kluwer, Dordrecht, pp. 592.
- Suyker, A.E. and Verma, S.B. (2001) Year-round observations of the net ecosystem exchange of carbon dioxide in a native tallgrass prairie. *Global Change Biol.* 7, 279–289.
- Wilson, K.B., Baldocchi, D.D. and Hanson, P.J. (2000) Spatial and seasonal variability of photosynthetic parameters and their relationship to leaf nitrogen in a deciduous forest. *Tree Physiol.* 20, 565–578.